Theoretical Study of O_2-H_2O: Potential Energy Surface, Molecular Vibrations, and Equilibrium Constant at Atmospheric Temperatures

Akiyoshi Sabu,[†] Satomi Kondo,[†] Ryu Saito,[‡] Yasuko Kasai,[‡] and Kenro Hashimoto*[,†]

Computer Center and Department of Chemistry, Tokyo Metropolitan University, 1-1 Minami-Ohsawa, Hachioji, Tokyo 192-0397, Japan, and Global Environment Division, Communications Research Laboratory, 4-2-1 Nukui-Kitamachi, Koganei, Tokyo 184-8795, Japan

Received: April 22, 2004; In Final Form: December 24, 2004

The intermolecular potential energy surface of O_2-H_2O was investigated at ab initio MP2 and MRSDCI levels using the aug-cc-pVTZ basis set. The vibrational levels were evaluated by numerically solving the Schrödinger equations for the nuclear motions with the ab initio potential functions using one- to three-dimensional finite-element methods. On the basis of the calculated partition functions, the equilibrium constant of the complex, K_p, was studied. The K_p values at atmospheric temperatures of 200−300 K were found to be 1−2 orders of magnitude less than previous estimates from the harmonic oscillator approximation.

1. Introduction

Binary complexes including a water molecule, such as HO_2-H_2O, O_3-H_2O, CH_4-H_2O, and O_2-H_2O, are attracting attention because they may work as a reservoir in the atmospheric chemical systems.[1−3] On the other hand, collision complexes of the major atmospheric gases such as the O_2 dimer are known to contribute to a significant part of the total budget of incoming solar radiation.[2,4] The effort to observe the bound dimers has been started, and the first detection of the water dimer, which forms a strong hydrogen bond, was reported recently in the atmosphere.[5]

The O_2-H_2O van der Waals (vdW) complex whose ground electronic state is triplet is an interesting research target, but its abundance in the atmosphere is not well-known. The abundance can be calculated using statistical and thermodynamic procedures,[1] which require spectroscopic data describing the rotational and vibrational partition functions to estimate the equilibrium constant, K_p. So far, there has been only one spectroscopic study for this complex. Kasai et al.[6] recorded the rotational spectrum of the complex by the Fourier transform microwave (FTMW) experiment in the laboratory. Theoretically, a few studies[1,7,8] were carried out to calculate the structure of the complex and estimate K_p by the harmonic oscillator approximation (HOA). However, it is easily noticed that the HOA may not be adequate to estimate K_p for the weakly bound complex. The vibrational partition functions by the HOA may include the contribution from the levels above the dissociation energy, giving rise to the overestimated K_p.

In the present work, the vibrational partition functions were examined by evaluating the anharmonic vibrational levels below the dissociation energy using the potential energy surface (PES) at the ab initio correlated levels to improve K_p for the O_2-H_2O in the previous studies.[1,7,8] The temperature dependence of K_p and the altitude dependence of the mixing ratio were investigated. The results will be a basis for a better understanding of the role of the water vapor complex in the Earth's atmosphere.

* Corresponding author. E-mail: hashimoto-kenro@c.metro-u.ac.jp. Fax: +81-426-77-1352.
[†] Tokyo Metropolitan University.
[‡] Communications Research Laboratory.

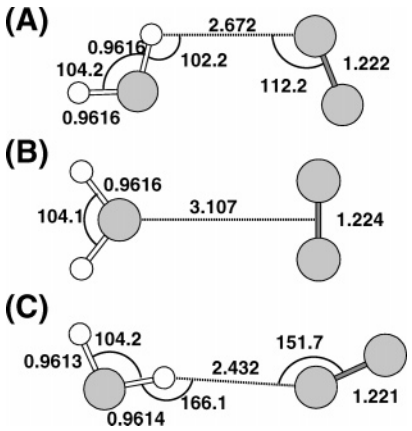

Figure 1. Optimized geometries of O_2-H_2O at the MP2/aug-cc-pVTZ level. The geometric parameters are given in angstroms and degrees.

2. Structures, Potential Energy Surface, and In-Plane Intermolecular Vibrations

We previously reported the geometries, the PES along the in-plane intermolecular coordinates, and the energies and wave functions of the four lowest states for the in-plane intermolecular vibrations of O_2-H_2O.[9] A brief summary is given here.

Representative low-energy structures are shown in Figure 1. They were optimized using the Gaussian-98 program[10] by the second-order Møller−Plesset perturbation method (MP2) with the usual frozen-core approximation with the aug-cc-pVTZ basis set.[11] The C_s structure, A, in which the O−O bond and the bisector line of the H−O−H angle of water are nearly parallel, is the global potential minimum. The electronic binding energy, ΔE, with and without the counterpoise correction[12] (CPC) for the basis set superposition error (BSSE) is −0.54 and −0.76 kcal/mol, respectively, with the latter being very close to the value at the QCISD/6-311++G(2d,2p) level (−0.72 kcal/mol).[7,13] The C_{2v} configuration, B, which is higher than A by only 0.06 (0.10) kcal/mol with (without) CPC, is a transition state for the in-plane disrotatory motion of the monomers connecting two equivalent A-type minima. The hydrogen-bonded linear form, C, is less stable than A by 0.21 (0.14) kcal/

10.1021/jp0482518 CCC: $30.25
Published on Web 02/09/2005

TABLE 1: Energy Levels of Intermolecular Modes[a]

in-plane vibrations		out-of-plane vibrations: bending			out-of-plane vibrations: torsion		
$\|\nu_c, \nu_d, \nu_s\rangle$	energy/cm^{-1}	$\|\nu_b\rangle$	energy/cm^{-1}		$\|\nu_t\rangle$	energy/cm^{-1}	
$\|0+, 0+, 0\rangle$	67.8[b]	(0.00)	$\|0\rangle$	24.8[b]	(0.00)	$\|0\rangle$	32.9[b]	(0.00)
$\|0-, 0+, 0\rangle$	67.8	(0.00)	$\|1\rangle$	72.7	(47.9)	$\|1\rangle$	36.5	(3.66)
$\|0+, 0-, 0\rangle$	74.7	(6.90)	$\|2\rangle$	102	(77.1)	$\|2\rangle$	73.8	(40.9)
$\|0-, 0-, 0\rangle$	74.7	(6.90)				$\|3\rangle$	103	(70.4)
$\|1+, 1+, 0\rangle$	83.8	(16.0)				$\|4\rangle$	107	(74.2)
$\|1-, 1+, 0\rangle$	84.2	(16.4)						
$\|1+, 1-, 0\rangle$	87.2	(19.4)						
$\|1-, 1-, 0\rangle$	88.6	(20.8)						
$\|2+, 2+, 0\rangle$	92.5	(24.7)						
$\|2-, 2+, 0\rangle$	95.5	(27.7)						

[a] The values in parentheses are from the lowest level. [b] ZPE.

mol. This structure is a transition state connecting the A-type minima through an A″-symmetry motion, though it is at a minimum at the MP2(full)/6-311++G(2d,2p) level.[8]

The PES along the in-plane intermolecular coordinates was explored using the multireference single- and double-excitation configuration interaction (MRSDCI) method,[14-16] preceded by the double-configuration self-consistent-field (DCSCF) calculations with the aug-cc-pVTZ basis set. The active space for the DCSCF consisted of the π_u and π_g orbitals in O_2, in which six electrons were distributed ($\pi_u^4\pi_g^2$ and $\pi_u^2\pi_g^4$ in O_2). The natural orbitals obtained by the DCSCF were used as one-particle functions in the MRSDCI calculations with the DCSCF reference. All the single and double excitations from the two reference configurations, except those from three 1s orbitals on the O atoms, were included. The size-consistency correction was included by Davidson's method.[17] The MOLPRO-2000 program[18] was used. The results of the MRSDCI calculations are essentially similar to those of the MP2 calculations. There are four equivalent A-type minima reflecting the periodic PES along the internal-rotation coordinates of the monomers. Their ΔE is -167 cm^{-1} (-0.48 kcal/mol); all energy values are given with CPC from here on, unless otherwise stated. The B- and C-type geometries are located only 25 cm^{-1} (0.07 kcal/mol) and 46 cm^{-1} (0.13 kcal/mol), respectively, above the A structures. The ΔE value for structure A with the Pople-type size-consistency correction[19] was -169 cm^{-1}, which was almost the same as that with Davidson's correction.

The in-plane intermolecular vibrations were examined by numerically solving the Schrödinger equations for the nuclear motions, whose potential function was taken from the MRSDCI calculations, using the finite-element method (FEM).[20,21] We developed this method and the program code to solve up to three-dimensional problems. The energy levels of the four lowest states for the in-plane intermolecular vibrations are given in Table 1, together with those of higher states below the dissociation limit we report in this work. In the labels of the form $|\nu_c, \nu_d, \nu_s\rangle$, ν_c and ν_d represent the quantum numbers for the conrotatory and disrotatory motions of the monomers, respectively, while ν_s represents the intermolecular stretching. The motions of these three modes are illustrated in Figure 2. The separations of the four lowest states reflect the PES, which is practically of the double-well type along both the conrotatory and disrotatory paths.[9] The $\nu_c = 0+$ and $\nu_c = 0-$ levels are actually degenerate, while the $\nu_d = 0+$ and $\nu_d = 0-$ levels are split by 6.9 cm^{-1}. The corresponding nuclear wave functions are characterized by the C_{2v} symmetry. These indicate the feasibility of disrotatory motion,[22] which is consistent with the FTMW spectrum where the molecular symmetry of the complex inferred from the hyperfine structure[6] is not C_s but C_{2v}.

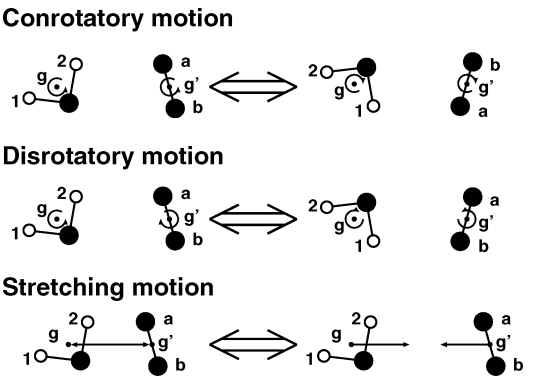

Figure 2. Schematic illustration of in-plane intermolecular modes: (a) conrotatory motions of the monomers; (b) disrotatory motions of the monomers; (c) intermolecular stretching. g and g′ represent the centers of mass for H_2O and O_2, respectively.

The intermolecular in-plane zero-point energy (ZPE) and the higher vibrational levels were examined. The ZPE including all contributions from the three modes was 67.8 cm^{-1}, which was less than the corresponding harmonic value at the MP2 level by 51.9 cm^{-1}. The higher levels corresponded to the excited states of the conrotatory and disrotatory motions, and no excited state was calculated for the intermolecular stretching below the dissociation energy (see Table 1).

3. Other Vibrations

3.1. Out-of-Plane Intermolecular Vibrations. In this study, the intermolecular out-of-plane bending and torsion were investigated by solving the following one-dimensional Schrödinger equations:

$$\left(-\frac{\hbar^2}{2I_b}\frac{d^2}{d\theta_b^2} + V(\theta_b)\right)\Psi(\theta_b) = E\Psi(\theta_b),\ I_b = 2m_H R_{gHb}^2 + m_O R_{gO}^2, \text{ for bending} \quad (1)$$

$$\left(-\frac{\hbar^2}{2I_t}\frac{d^2}{d\theta_t^2} + V(\theta_t)\right)\Psi(\theta_t) = E\Psi(\theta_t),\ I_t = 2m_H R_{gHt}^2, \text{ for torsion} \quad (2)$$

The angular variables as well as the distance parameters are shown in Figures 3 and 4. The potential functions were computed at the MRSDCI level with the aug-cc-pVTZ basis set and evaluated by changing θ_b (θ_t) at intervals of 15° (10°). At the given θ_b (θ_t), the energies were calculated by varying the intermolecular distance, $R_{gg'}$, with all other inter- and intramolecular parameters fixed to those at the A-type minimum. The minimum energies with respect to $R_{gg'}$ for each given θ_b (θ_t) were used to construct $V(\theta_b)$ ($V(\theta_t)$). m_H and m_O in the moments of inertia, I_b and I_t, are the masses of hydrogen and oxygen, respectively. The FEM was used with sixth-order Lagrange interpolation polynomials placed at 10 equally spaced points for each coordinate, and the periodic boundary conditions $\Psi(\theta_b + 2\pi) = \Psi(\theta_b)$ and $\Psi(\theta_t + 2\pi) = \Psi(\theta_t)$ were applied.

The potential energy curves (PECs), vibrational levels, and wave functions for the out-of-plane modes are illustrated in Figures 3 and 4. The energies of the levels are summarized in Table 1. The PEC for the bending had a single barrier at $\theta_b = \pm 180°$, which was 111 cm^{-1} from the bottom; three vibrational states were lower than the barrier. The calculated intermolecular bending ZPE and fundamental frequencies were 24.8 and 47.9 cm^{-1}, respectively, with the latter being much lower than the

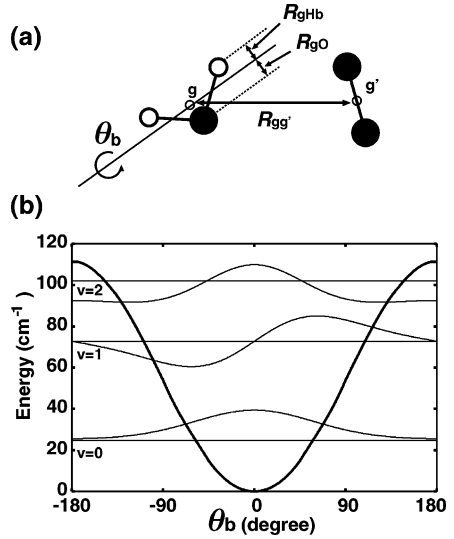

Figure 3. (a) Geometric parameters in the Schrödinger equation for intermolecular out-of-plane bending. g and g′ represent the centers of mass for H_2O and O_2, respectively. R_{gHb} and R_{gO} are 0.5205 and 0.065 60 Å, respectively. (b) Potential energy curve by the MRSDCI method and energy levels and wave functions for low-lying vibrational states.

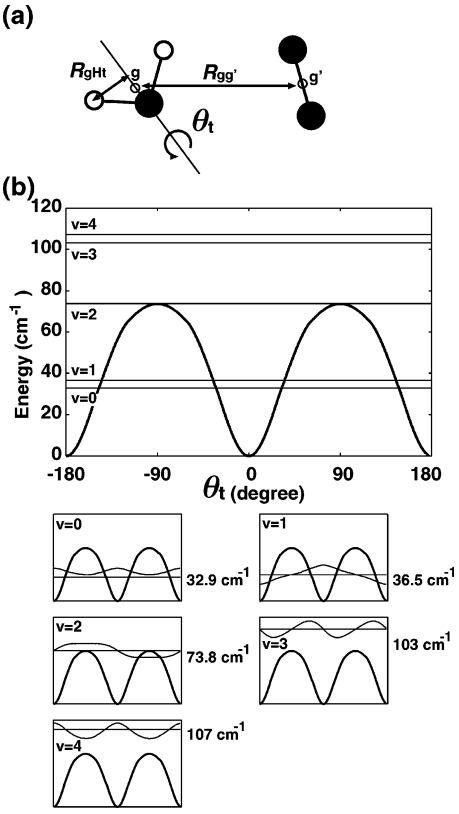

Figure 4. (a) Geometric parameters in the Schrödinger equation for intermolecular torsion. g and g′ represent the centers of mass for H_2O and O_2, respectively. R_{gHt} is 0.7570 Å. (b) Potential energy curve by the MRSDCI method and energy levels and wave functions for low-lying vibrational states.

harmonic frequency at the MP2 level (87.9 cm^{-1}). The ZPE of the intermolecular torsion (32.9 cm^{-1}) was about half the corresponding harmonic value at the MP2 level (66.9 cm^{-1}). The two lowest levels were split by ≈4 cm^{-1}, reflecting the double-well PEC with barriers of 74 cm^{-1} at $\theta_t = \pm 90°$. The very low energy of the $\nu_t = 1$ state could be regarded as being the result of the large separation of the internal rotational levels with $\nu_t = 1$ and 2. As Table 1 shows, the frequencies of even the high overtones of the intermolecular modes were less than those for the so-called window region of the atmosphere (∼800− 1200 cm^{-1}).

TABLE 2: Energy Levels of Intramolecular Modes in Complex and Free States

Complex

H_2O			O_2		
label $\|\nu_1, \nu_2, \nu_3\rangle$	anharmonic energy/cm^{-1}	harmonic[a] energy/cm^{-1}	label $\|\nu\rangle$	anharmonic energy/cm^{-1}	harmonic[a] energy/cm^{-1}
$\|0, 0, 0\rangle$	4686(0)	4686(0)	$\|0\rangle$	820(0)	846(0)
$\|0, 1, 0\rangle$	6291(1605)	6295(1609)	$\|1\rangle$	2443(1622)	2538(1692)

Free State

H_2O			O_2		
label $\|\nu_1, \nu_2, \nu_3\rangle$	anharmonic energy/cm^{-1}	harmonic[a] energy/cm^{-1}	label $\|\nu\rangle$	anharmonic energy/cm^{-1}	harmonic[a] energy/cm^{-1}
$\|0, 0, 0\rangle$	4694(0)	4699(0)	$\|0\rangle$	799(0)	728(0)
$\|0, 1, 0\rangle$	6293(1599)	6327(1628)	$\|1\rangle$	2381(1581)	2183(1455)
$\|0, 2, 0\rangle$	7845(3151)		$\|2\rangle$	3940(3140)	
$\|1, 0, 0\rangle$	8447(3753)	8521(3822)	$\|3\rangle$	5476(4677)	
$\|0, 0, 1\rangle$	8528(3834)	8647(3948)	$\|4\rangle$	6990(6190)	
$\|0, 3, 0\rangle$	9586(4892)		$\|5\rangle$	8481(7682)	
$\|1, 1, 0\rangle$	10029(5335)				
$\|0, 1, 1\rangle$	10105(5411)				
$\|0, 4, 0\rangle$	11046(6352)				
$\|1, 2, 0\rangle$	11575(6881)				
$\|0, 2, 1\rangle$	11658(6964)				
$\|2, 0, 0\rangle$	12160(7466)				
$\|1, 0, 1\rangle$	12212(7518)				
$\|0, 0, 2\rangle$	12321(7627)				

[a] At the MP2/aug-cc-pVTZ level.

3.2. Intramolecular Vibrations. The intramolecular frequencies of O_2 and H_2O in the complex and isolated states were examined. The PEC along the O_2 bond in the complex was calculated using the same MRSDCI method. The O_2 distance was varied while keeping the other geometric parameters fixed to those of the potential minimum. The PES along two OH stretches and an HOH bending was explored in a similar way, but the MP2 method was used to adequately consider the electron correlation in water. The frequencies of the intramolecular vibrations were much higher than those of the intermolecular modes and showed very small changes upon complex formation. Therefore, the partition functions for the intramolecular modes should have a slight effect on the equilibrium constant, which will be discussed later. With these potential energy functions, the vibrational levels and corresponding nuclear wave functions were obtained by solving the one (O_2)- and three (H_2O)-dimensional Schrödinger equations by the FEM.

The calculated energy levels of the intramolecular modes are listed in Table 2. The energies of the ground and first excited states by the HOA are given for comparison. All of the fundamental frequencies by the present anharmonic calculation were in good agreement with the experimental values for both O_2 (1556 cm^{-1}) and H_2O (3657(ν_1), 1595(ν_2), and 3756(ν_3) cm^{-1}).[23] They were almost unchanged in the complex state, though the O_2 stretching and HOH bending frequencies were slightly higher, reflecting the mutual orientations of the monomers. The calculated anharmonic zero-point energies for both monomers agreed well with the experimental ones (787 cm^{-1} (O_2)[23] and 4634 cm^{-1} (H_2O)[24]).

4. Equilibrium Constant

4.1. Computational Details. With the Born−Oppenheimer approximation, and ignoring the vibrational−rotational coupling,

the equilibrium constant, K_p (Pa^{-1}), for O_2-H_2O is expressed by

$$K_p = \frac{Q^t_{O_2-H_2O}}{Q^t_{O_2} Q^t_{H_2O}} \frac{Q^r_{O_2-H_2O}}{Q^r_{O_2} Q^r_{H_2O}} \frac{Q^v_{O_2-H_2O}}{Q^v_{O_2} Q^v_{H_2O}} \exp\left(-\frac{hc\Delta E_{zpc}}{kT}\right) \frac{1}{kT} \quad (3)$$

Here, the symbol Q^t_M is the translational partition function per unit volume and Q^r_M and Q^v_M are the rotational and vibrational partition functions for the complex ($M = O_2-H_2O$) as well as the isolated monomers ($M = O_2$ and H_2O). The exponential part is derived from the electronic partition function, and h, c, ΔE_{zpc}, k, and T are the Planck constant ($6.626\,075\,5 \times 10^{-34}$ J·s), the light velocity in a vacuum ($2.997\,924\,58 \times 10^{10}$ cm·s^{-1}), the binding energy with a zero-point correction (cm^{-1}), the Boltzmann constant ($1.380\,658 \times 10^{-23}$ J·K^{-1}), and the temperature (K), respectively.

The translational and rotational partition functions for both the complex and isolated states were calculated using the usual textbook formulas.[25] The rotational constants of each monomer were taken from the structures at the dissociation limit by the MRSDCI method.[9] They were 43.70 GHz (B) for O_2 and 821.9 (A), 437.6 (B), and 285.6 (C) GHz for H_2O. Their deviations from the experimental values were at most 3%. The symmetry number of the molecular rotation was 2 for each monomer.

In the complex, the in-plane disrotatory motion of monomers is feasible as mentioned and the ground-state wave functions for this mode are delocalized.[9] Thus, the rotational constants of the complex were not calculated using the C_s potential-minimum structure but evaluated from the expectation value of the moment of inertia for the lowest $|0+, 0+, 0\rangle$ and $|0-, 0+, 0\rangle$ states. They were 44.02 (A), 3.536 (B), and 3.273 (C) GHz. The calculated $^1/_2(B + C)$ value deviated from the experimental value (3.633 GHz)[6] by 6%. Changes in these constants in the rotational and vibrational excited states were not included. The symmetry number of the molecular rotation was 1 for the complex.

The vibrational partition function is the sum of the Boltzmann factors over all bound states:

$$Q^v_M = \frac{1}{\sigma_v} \sum_{i=0}^{N} \exp\left(-\frac{hc\epsilon_i}{kT}\right) \quad (M = O_2, H_2O, \text{and } O_2-H_2O) \quad (4)$$

where σ_v is the symmetry number for the internal rotations, ϵ_i is the energy of the ith vibrational level (cm^{-1}) from the zero-point level, and N corresponds to the upper limit of the bound states.

σ_v was 1 for each monomer. Since the intermolecular vibrational levels were obtained using the global PES with the multiple equivalent minima, the symmetry number for the internal rotation, which was 2 for both O_2 and H_2O in the complex, was taken into account when calculating the partition functions. The total symmetry number was 4 in the complex due to the internal rotations, while that of the monomer state was 4 due to the molecular rotations.

For the free monomers, those levels lower than the first electronic excited state of O_2 (7918 cm^{-1})[23] were included; these are listed in Table 2. The contribution of the highest level considered (7682 cm^{-1} (O_2) and 7627 cm^{-1} (H_2O)) to the total vibrational partition function computed by including up to these states was around 10^{-14}% for both monomers, so further high states were ignored.

TABLE 3: Energies of Bound States[a] Used in the Calculation of K_p^{anh}

$\|\nu_c, \nu_d, \nu_s\rangle\|\nu_b\rangle\|\nu_t\rangle$	energy[a]/cm^{-1}	$\|\nu_c, \nu_d, \nu_s\rangle\|\nu_b\rangle\|\nu_t\rangle$	energy[a]/cm^{-1}
$\|0+, 0+, 0\rangle\|0\rangle\|0\rangle$	0.00	$\|1+, 1-, 0\rangle\|0\rangle\|0\rangle$	19.4
$\|0-, 0+, 0\rangle\|0\rangle\|0\rangle$	0.00	$\|1+, 1+, 0\rangle\|0\rangle\|1\rangle$	19.7
$\|0+, 0+, 0\rangle\|0\rangle\|1\rangle$	3.66	$\|1-, 1+, 0\rangle\|0\rangle\|1\rangle$	20.1
$\|0-, 0+, 0\rangle\|0\rangle\|1\rangle$	3.66	$\|1-, 1-, 0\rangle\|0\rangle\|0\rangle$	20.8
$\|0+, 0-, 0\rangle\|0\rangle\|0\rangle$	6.90	$\|1+, 1-, 0\rangle\|0\rangle\|1\rangle$	23.1
$\|0-, 0-, 0\rangle\|0\rangle\|0\rangle$	6.90	$\|1-, 1-, 0\rangle\|0\rangle\|1\rangle$	24.5
$\|0+, 0-, 0\rangle\|0\rangle\|1\rangle$	10.6	$\|2+, 2+, 0\rangle\|0\rangle\|0\rangle$	24.7
$\|0-, 0-, 0\rangle\|0\rangle\|1\rangle$	10.6	$\|2-, 2+, 0\rangle\|0\rangle\|0\rangle$	27.7
$\|1+, 1+, 0\rangle\|0\rangle\|0\rangle$	16.0	$\|2+, 2+, 0\rangle\|0\rangle\|1\rangle$	28.4
$\|1-, 1+, 0\rangle\|0\rangle\|0\rangle$	16.4		

[a] ϵ_i in eq 4.

For the binary complex, the vibrational levels below the dissociation energy were included straightforwardly when evaluating the partition functions. In the present case, the binding energy with ZPE, ΔE_{ZPC}, was only -28.6 cm^{-1} (-0.08 kcal/mol), mainly because of the contribution from the intermolecular vibrations. Thus, a total of 19 states, whose energies are listed in Table 3, were actually used. They corresponded to the combinations of the ground and low-lying excited states of the intermolecular vibrations examined in the previous section. The excited levels for all of the intramolecular vibrations were excluded from the calculation of K_p because their fundamental frequencies exceeded the dissociation energy. The contribution of states above the dissociation energy to the partition function was recently discussed in relation to water dimers.[26] It is beyond the scope of this paper to consider these short-lived dissociative states.

The sensitivity of K_p to the (de)coupling methods of the intermolecular modes was tested. The order of magnitude of K_p did not depend on the form of the (de)coupling in the 200–300 K region, though the absolute values changed to some extent. The dependence of the electronic binding energy and K_p on the levels of the molecular orbital (MO) calculations was examined. The deviation of the electronic binding energy from that at the MRSDCI/aug-cc-pVTZ level was at most $\sim$40 cm^{-1} (0.12 kcal/mol) at the MP2/aug-cc-pVQZ level. However, the order of magnitude of K_p was not changed by the level of the MO calculations at 200 and 300 K. The results of these tests are summarized in the Supporting Information (Appendices IS and IIS and Tables IS and IIS).

We calculated K_p using the optimized geometry and harmonic frequencies at the MP2 level, designating it as K_p^{har}. The vibrational partition function with the HOA is usually given by

$$Q^v_M = \prod_{i=1}^{NF} \left(1 - \exp\left(-\frac{hc\tilde{\nu}_i}{kT}\right)\right)^{-1} \quad (M = O_2, H_2O, \text{and } O_2-H_2O) \quad (5)$$

where $\tilde{\nu}_i$ is the harmonic frequency of the ith normal mode and NF is the number of degrees of freedom. Experimental frequencies were used for the monomers, while scaled frequencies were employed for each intramolecular mode in the complex. The scale factors were determined by the ratio between the experimental and calculated harmonic frequencies for each mode. The intermolecular harmonic frequencies were used without scaling. The frequencies used in computing K_p^{har} are listed in Table 4. The symmetry number for the C_s-symmetry binary complex was 1.

4.2. Temperature Dependence of K_p. Figure 5 illustrates the equilibrium constant as a function of temperature for both

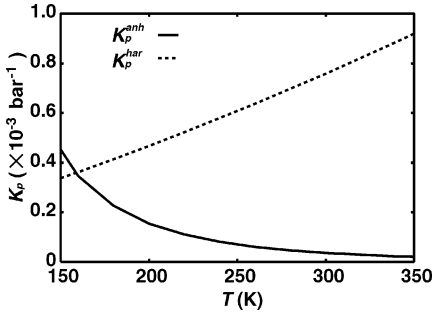

Figure 5. Equilibrium constant (bar^{-1}) as a function of temperature (K) by anharmonic, K_p^{arh}, and harmonic, K_p^{har}, treatments.

TABLE 4: Frequencies Used in the Calculation of K_p^{har}

O_2/cm^{-1}		H_2O/cm^{-1}			O_2-H_2O/cm^{-1}	
exptl	(ab initio)	exptl	(ab initio)	scale factor	scaled	(ab initio)
						(39.95)
						(85.76)
						(87.90)
						(113.6)
						(133.7)
1556	(1455)			1.069	1809	(1692)
		1595	(1628)	0.9797	1576	(1609)
		3657	(3822)	0.9568	3653	(3818)
		3756	(3948)	0.9514	3752	(3944)

TABLE 5: Equilibrium Constants at T = 200, 220, 240, 260, 280, and 300 K

	present work[a]		Vaida and Headrick[b]	Kjaergaard et al.[c]
T/K	K_p^{anh}/bar^{-1}	K_p^{har}/bar^{-1}	K_p^{har}/bar^{-1}	K_p^{har}/bar^{-1}
200	1.72×10^{-4}	4.61×10^{-4}	2.23×10^{-3}	4.12×10^{-3}
220	1.22×10^{-4}	5.15×10^{-4}	2.46×10^{-3}	4.08×10^{-3}
240	8.95×10^{-5}	5.71×10^{-4}	2.69×10^{-3}	4.09×10^{-3}
260	6.72×10^{-5}	6.28×10^{-4}	2.93×10^{-3}	4.13×10^{-3}
280	5.15×10^{-5}	6.87×10^{-4}	3.18×10^{-3}	4.20×10^{-3}
300	4.03×10^{-5}	7.47×10^{-4}	3.44×10^{-3}	4.29×10^{-3}

[a] With CPC. [b] At the MP2(full)/6-311++G(2d,2p) level without CPC for a C-type structure. [c] At the QCISD/6-311++G(2d,2p) level without CPC for an A-type structure.

the present anharmonic treatment, K_p^{anh}, and the harmonic one, K_p^{har}. The values of K_p^{anh} and K_p^{har} at several temperatures are listed in Table 5.

The values of K_p^{anh} at 150−350 K at intervals of 5 K are given in the Supporting Information (Table IIIS). K_p^{anh} decreased from 1.72×10^{-4} bar^{-1} (1.75×10^{-4} atm^{-1}) to 4.03×10^{-5} bar^{-1} (4.08×10^{-5} atm^{-1}) in the 200−300 K region, reflecting the dissociation of the complex, while K_p^{har} showed the opposite temperature dependence. K_p^{har} was about 3 and 20 times larger than K_p^{anh} at 200 and 300 K, respectively. There are two reasons for the unusual behavior of K_p^{har}. One was the positive binding energy, ΔE_{ZPC}, 155 cm^{-1} (0.44 kcal/mol), due to the overestimated intermolecular frequencies, which resulted in a rise in K_p^{har} with increasing temperature. The other is that K_p^{har} based on the partition functions from eq 5 included the contribution of an infinite number of high levels over the dissociation energy.

Let us now state briefly what can be learned from K_p^{har} in previous studies,[1,7] whose values are listed in Table 5. They are plotted against temperature together with K_p^{anh} and K_p^{har} from the present study in Figure 1S in the Supporting Information.[27] Vaida and Headrick[1] first estimated the abundance of O_2-H_2O in the atmosphere based on K_p^{har}. They used a linear C-type geometry and harmonic frequencies at the MP2(full)/6-311++G(2d,2p) level.[8] However, after a careful examination of the energetics, we found that ΔE_{zpc} was positive (94.9 cm^{-1} (0.27 kcal/mol)) for this structure, which was in conflict with the experimental detection of the complex. As a result, their K_p^{har} values increased monotonically as temperature increased. Kjaergaard et al.[7] computed K_p^{har} for the A-like global minimum at the QCISD/6-311++G(2d,2p) level by using ΔE_{zpc} without CPC (−51.2 cm^{-1} (−0.15 kcal/mol)), though they were interested not only in the abundance but also in the intensity of the OH stretch overtones in the complex. Because of the small but negative ΔE_{zpc} value, their K_p^{har} as a function of temperature decreased to $\approx 4.1 \times 10^{-3}$ bar^{-1} at 227 K and then increased very gradually at higher temperatures, reaching $\approx 4.3 \times 10^{-3}$ bar^{-1} at 300 K due to the overestimated vibrational partition function of the complex.

Here, we examined K_p^{anh} by the present procedure using the PES without CPC, since the counterpoise method may overestimate the magnitude of the BSSE. The K_p^{anh} values without CPC are listed in the Supporting Information (Table IIIS). The ΔE_{zpc} without CPC was −62.8 cm^{-1}, and the number of bound states was 87. The rotational constants for the structure without CPC were 51.98 (A), 3.390 (B), and 3.183 (C) GHz. The K_p^{anh} without CPC, which may be viewed as the maximum estimate, was about 5 times larger than that with CPC at 200−300 K. Nevertheless, the equilibrium constant, taking into account the anharmonic PES and the dissociation of the complex, was less than $^1/_{10}$ of the previous estimates based on the HOA.[1,7]

4.3. Comparison with the Water Dimer. There may be some concerns about our K_p^{anh} value for O_2-H_2O, which was smaller than K_p^{har}, because it is known that the K_p^{har} value for the water dimer is less than about one-third of the experimental equilibrium constant, K_p^{exp}, at 373 K.[7]

From eq 3, the value of K_p^{har}/K_p^{exp} is considered to be determined mostly by the ratio of the harmonic partition function over the actual one for intermolecular vibrations, $Q_{int}^{har}/Q_{int}^{exp}$. It was found that ∼40% of K_p^{har}, and thus Q_{int}^{har}, for the water dimer was from states above the dissociation energy at 373 K for the QCISD/6-311++G(2d,2p) level. Nevertheless, the theoretical Q_{int}^{har} value is likely to be much smaller than the true value due to the underestimated density of states for this hydrogen-bonded complex. Since ΔE amounts to ∼5 kcal/mol,[28,29] there should actually be a greater number of bound states than that expected from the HOA. However, the large separations between the harmonic levels probably gave rise to a serious underestimation of the number of bound states. In fact, the equilibrium constant evaluated by taking low anharmonic intermolecular frequencies as well as bound levels into account is larger than K_p^{har} at 373 K and agrees well with experimental results,[29,30] strongly supporting this conclusion.

In O_2-H_2O, because of the small binding energy, the number of bound states, and thus the anharmonic partition functions of the intermolecular vibrations, Q_{int}^{anh}, was very small. On the other hand, Q_{int}^{har} was vastly overestimated. Indeed, we found that more than 99% of Q_{int}^{har} was from states above the dissociation energy at 300 K at the QCISD/6-311++G(2d,2p) level. Consequently, it follows that K_p^{anh} was much less than K_p^{har} for O_2-H_2O in contrast to the water dimer, and the small binding energy was responsible for this difference.

5. Mixing Ratio

On the basis of the present K_p^{anh} value with CPC, the altitude dependence of the volume mixing ratio (vmr) for O_2-H_2O was

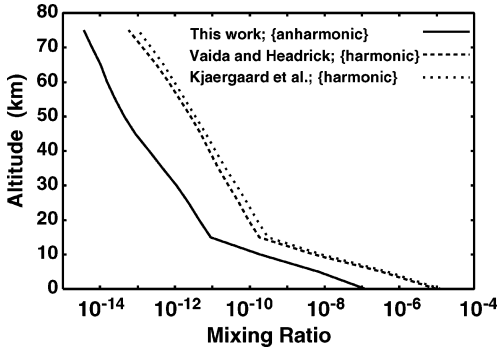

Figure 6. Altitude dependence of mixing ratio (vmr) for O_2-H_2O by K_p^{arh} (solid line) together with those by harmonic treatment from Vaida and Headrick (2000) (dashed line) and Kjaergaard et al. (2003) (dotted line).

studied up to 75 km at intervals of 5 km using

$$\left(\frac{P_{O_2-H_2O}}{P}\right) = K_p^{anh} P \left(\frac{P_{O_2}}{P}\right)\left(\frac{P_{H_2O}}{P}\right) \quad (6)$$

Here, P is the atmospheric pressure at each altitude and P_M (M = O_2-H_2O, O_2, and H_2O) is the partial pressure of the complex and monomers. The results are shown in Figure 6. The K_p^{anh} values used to draw this figure are given in the Supporting Information (Table IVS). For the atmospheric pressure, P, and the temperature in K_p^{anh} at each altitude, the standard values for the midlatitudes[31] were used. The altitude dependence in the mixing ratio of water, P_{H_2O}/P, was from the literature,[31] while that of oxygen, P_{O_2}/P, was assumed to be constant at 20.95% for all altitudes. These conditions were the same as those used in previous studies.[1,7] The mixing ratios of the complex evaluated using the literature K_p^{har} values[1,7] were plotted for comparison.

$P_{O_2-H_2O}/P$ by the present K_p^{anh} value at the ground level was $\approx 1.37 \times 10^{-7}$, decreasing rapidly to $\approx 1.02 \times 10^{-11}$ at the tropopause (15−16 km). The remarkable drop can be attributed mainly to P_{H_2O}/P, which decreased by about 4 orders of magnitude in the troposphere, since the variations in both P and K_p^{anh} were less than 1 order of magnitude. $P_{O_2-H_2O}/P$ decreased further but at a slower rate above the troposphere, becoming $\approx 4.87 \times 10^{-14}$ at the stratopause (50 km). The relatively gentle slope above the troposphere is mostly determined by the altitude dependence of P; K_p^{anh} decreased slightly in the corresponding temperature region, while P_{H_2O}/P was nearly constant in the stratosphere and mesosphere compared with that in the troposphere.

Note that the present mixing ratio was about 1−2 orders of magnitude less than those by K_p^{har} in the previous studies[1,7] at the ground level, but the plots of the mixing ratio by K_p^{anh} and K_p^{har} change roughly in parallel with each other from the surface level to 75 km. The mixing ratio of water, P_{H_2O}/P, is the dominant contributor to the mixing ratio of the O_2-H_2O complex, $P_{O_2-H_2O}/P$, in the troposphere, while $P_{O_2-H_2O}/P$ is mostly governed by the atmospheric pressure in the stratosphere and mesosphere.

6. Conclusion

In this work, the potential energy surface, molecular vibrations, and equilibrium constant of O_2-H_2O were studied theoretically. One- to three-dimensional finite-element methods were used to numerically solve the Schrödinger equations for the nuclear motions, whose potential functions were calculated at the ab initio MRSDCI and MP2 levels with the aug-cc-pVTZ basis set.

The intermolecular PES was very flat and strongly anharmonic. It is thus essential to treat intermolecular vibration beyond the harmonic oscillator approximation. The fundamental frequency of the intermolecular modes was at most ≈ 50 cm^{-1} for the out-of-plane bending, and no transition was found in the window region of the atmosphere.

By using the partition functions based on the anharmonic vibrational levels, the equilibrium constant, K_p, was evaluated. Though a more elaborate effort such as the inclusion of the full couplings among vibrations and the vibrational−rotational interactions may further improve K_p, it is worth emphasizing that the monotonic decrease of K_p with increasing temperature was obtained for the first time for O_2-H_2O by the present procedure. The estimated K_p^{anh} value was 1−2 orders of magnitude less than the K_p^{har} values in the previous studies at 200−300 K. The volume mixing ratio of the complex, $P_{O_2-H_2O}/P$, by the present K_p^{anh} value was smaller by the same order of magnitude than those by the K_p^{har} values at the ground level. $P_{O_2-H_2O}/P$ is mainly determined by the mixing ratio of water in the troposphere, while $P_{O_2-H_2O}/P$ is mostly governed by the atmospheric pressure in the stratosphere and mesosphere.

Acknowledgment. This work was supported in part by a grant-in-aid from the Ministry of Education, Culture, Sports, Science and Technology of Japan (MEXT). Some of the computations were carried out at the Research Center for Computational Science at the Okazaki National Research Institutes. K.H. is grateful for support from the Japanese Science and Technology Corporation (ACT-JST).

Supporting Information Available: Results of a test of the sensitivity of K_p^{anh} to the (de)coupling methods of the intermolecular modes (Appendix IS and Table IS), results of a test of the sensitivity of the electronic binding energy and K_p^{anh} to the levels of molecular orbital calculations (Appendix IIS and Table IIS), lists of the equilibrium constants (Tables IIIS and IVS), and plots of the equilibrium constants as a function of temperature (Figure 1S). This material is available free of charge via the Internet at http://pubs.acs.org.

References and Notes

(1) Vaida, V.; Headrick, J. E. *J. Phys. Chem. A* **2000**, *104*, 5401.
(2) Solomon, S.; Portmann, R. W.; Sanders, R. W.; Daniel, J. S. *J. Geophys. Res.* **1998**, *103*, 3847.
(3) Kasai, Y. *J. Spectrosc. Soc. Jpn.* **2000**, *49*, 200.
(4) Zender, C. S. *J. Geophys. Res.* **1999**, *104*, 24471.
(5) Pfeilsticker, K.; Lotter, C.; Peters, A.; Boesch, H. *Science* **2003**, *300*, 2078.
(6) Kasai, Y.; Sumiyoshi, Y.; Endo, Y. Presented at the 55th International Symposium on Molecular Spectroscopy, Ohio State University, Columbus, OH, 2000. Kasai, Y.; Saito R.; Sumiyoshi, Y.; Endo, Y. To be published.
(7) Kjaergaard, H. G.; Robinson, T. W.; Howard, D. L.; Daniel, J. S.; Headrick, J. E.; Vaida, V. *J. Phys. Chem. A* **2003**, *107*, 10680.
(8) Svishchev, I. M.; Boyd, R. J. *J. Phys. Chem. A* **1998**, *102*, 7294.
(9) Sabu, A.; Kondo, S.; Miura, N.; Hashimoto, K. *Chem. Phys. Lett.* **2004**, *391*, 101.
(10) Frisch, M. J.; Trucks, G. W.; Schlegel, H. B.; Scuseria, G. E.; Robb, M. A.; Cheeseman, J. R.; Zakrzewski, V. G.; Montgomery, J. A., Jr.; Stratmann, R. E.; Burant, J. C.; Dapprich, S.; Millam, J. M.; Daniels, A. D.; Kudin, K. N.; Strain, M. C.; Farkas, O.; Tomasi, J.; Barone, V.; Cossi, M.; Cammi, R.; Mennucci, B.; Pomelli, C.; Adamo, C.; Clifford, S.; Ochterski, J.; Petersson, G. A.; Ayala, P. Y.; Cui, Q.; Morokuma, K.; Rega, N.; Salvador, P.; Dannenberg, J. J.; Malick, D. K.; Rabuck, A. D.; Raghavachari, K.; Foresman, J. B.; Cioslowski, J.; Ortiz, J. V.; Baboul, A. G.; Stefanov, B. B.; Liu, G.; Liashenko, A.; Piskorz, P.; Komaromi, I.;

Gomperts, R.; Martin, R. L.; Fox, D. J.; Keith, T.; Al-Laham, M. A.; Peng, C. Y.; Nanayakkara, A.; Challacombe, M.; Gill, P. M. W.; Johnson, B.; Chen, W.; Wong, M. W.; Andres, J. L.; Gonzalez, C.; Head-Gordon, M.; Replogle, E. S.; Pople, J. A. *Gaussian 98*, revision A.11; Gaussian, Inc.: Pittsburgh, PA, 2001.

(11) Dunning, T. H., Jr. *J. Chem. Phys.* **1989**, *90*, 1007.

(12) Boys, S. F.; Bernardi, F. *Mol. Phys.* **1970**, *19*, 553.

(13) Kjaergaard, H. G.; Low, G. R.; Robinson, T. W.; Howard, D. L. *J. Phys. Chem. A* **2002**, *106*, 8955.

(14) Knowles, P. J.; Werner, H.-J. *Theor. Chim. Acta* **1992**, *84*, 95.

(15) Werner, H.-J.; Knowles, P. J. *J. Chem. Phys.* **1985**, *82*, 5053.

(16) Knowles, P. J.; Werner, H.-J. *Chem. Phys. Lett.* **1985**, *115*, 259.

(17) Langhoff, S. R.; Davidson, E. R. *Int. J. Quantum Chem.* **1974**, *8*, 61.

(18) MOLPRO is a package of ab initio programs written by Werner, H.-J.; Knowles, P. J. with contributions from Amos, R. D.; Bernhardsson, A.; Berning, A.; Celani, P.; Cooper, D. L.; Deegan, M. J. O.; Dobbyn, A. J.; Eckert, F.; Hampel, C.; Hetzer, G.; Korona, T.; Lindh, R.; Lloyd, A. W.; McNicholas, S. J.; Mandy, F. R.; Meyer, W.; Mura, M. E.; Nicklass, A.; Palmieri, P.; Pitzer, R.; Rauhut, G.; Schütz, M.; Stoll, H.; Stone, A. J.; Tarroni, R.; Thorsteinsson, T.

(19) Pople, J. A.; Seeger, R.; Krishnan, R. *Int. J. Quantum Chem. Symp.* **1977**, *11*, 149.

(20) Kimura, T.; Sato, S.; Iwata, S. *J. Comput. Chem.* **1988**, *9*, 827.

(21) Sato, N.; Iwata, S. *J. Comput. Chem.* **1988**, *9*, 222.

(22) Bunker, P. R.; Jensen, P. *Molecular Symmetry and Spectroscopy*, 2nd ed.; NRC Research Press: Ottawa, ON, Canada, 1998.

(23) Herzberg, G. *Molecular Spectra and Molecular Structure II. Infrared and Raman Spectra of Polyatomic Molecules*; Van Nostrand Reinhold: New York, 1945.

(24) Plíva, J.; Špirko V.; Papoušek D. *J. Mol. Spectrosc.* **1967**, *23*, 331.

(25) McQuarrie, D. A.; Simon, J. D. *Physical Chemistry A Molecular Approach*; University Science Books: Sausalito, CA, 1997.

(26) Schenter, G. K.; Kathmann, S. M.; Garrett, B. C. *J. Phys. Chem. A* **2002**, *106*, 1557.

(27) The spin multiplicity of the complex seems to be treated as singlet by Vaida and Headrick,[1] while that of the monomer O_2, as triplet. The original data for K_p in this reference were tripled and are used in Table 5 and Supporting Information Figure 1S.

(28) Curtiss, L. A.; Frurip, D. J.; Blander, M. *J. Chem. Phys.* **1979**, *71*, 2703.

(29) Goldman, N.; Fellers, R. S.; Leforestier, C.; Saykally, R. J. *J. Phys. Chem. A* **2001**, *105*, 515.

(30) Goldman, N.; Leforestier, C.; Saykally, R. J. *J. Phys. Chem. A* **2004**, *108*, 787.

(31) Brasseur, G.; Solomon, S. *Aeronomy of the Middle Atmosphere*, 2nd ed.; D. Reidel Publishing Company: Dordrecht, The Netherlands, 1986.